

Cell-Type-Specific Organization of Nuclear DNA Into Structural Looped Domains

Claudia Trevilla-García and Armando Aranda-Anzaldo*

Laboratorio de Biología Molecular, Facultad de Medicina, Universidad Autónoma del Estado de México, Paseo Tollocan y Jesús Carranza s/n, Toluca, 50180 Edo. Méx., Mexico

ABSTRACT

In the interphase nucleus of metazoan cells the DNA is organized in supercoiled loops anchored to a proteinaceous substructure known as the nuclear matrix (NM). The DNA is anchored to the NM by means of non-coding sequences of variable length known as matrix attachment regions or MARs operationally classified in structural-constitutive, resistant to high-salt extraction and transient-functional, non-resistant to high-salt extraction. The former are also known as true loop attachment regions or LARs that determine structural DNA loops. The DNA–NM interactions define a higher order structure within the cell nucleus (NHOS). We studied in a comparative fashion the NHOS in two primary cell types from the rat: hepatocytes and naive B lymphocytes, by analyzing the topological relationships between the NM and a set of eight short gene sequences located in six separate chromosomes and as such representing a coarse-grained, large-scale sample of the actual organization of nuclear DNA into structural loop domains. Our results indicate that such an organization is cell-type specific since most of the gene sequences studied showed significant differences in their relative position to the NM according to cell type. Such cell-type specific differences in the NHOS have no obvious correlation with the tissue-specific transcriptional activity of the corresponding genes, supporting the notion that permanent, structural DNA loops are different from transient, functional DNA loops that may be associated with transcription. *J. Cell. Biochem.* 112: 531–540, 2011. © 2010 Wiley-Liss, Inc.

KEY WORDS: B LYMPHOCYTE; HEPATOCYTE; LOOP ATTACHMENT REGION; MATRIX ATTACHMENT REGION; NUCLEAR MATRIX; NUCLEOTYPE

In the interphase nucleus of metazoan cells the DNA is organized in supercoiled loops anchored to a nuclear substructure commonly known as the nuclear matrix (NM) that is a non-soluble complex of ribonucleoproteins obtained after extracting the nucleus with non-ionic detergents, high salt, and treatment with DNase [Nickerson, 2001; Tsutsui et al., 2005]. The exact composition of the NM is a matter of debate as some 400 proteins have been associated with this structure [Mika and Rost, 2005]. The DNA is anchored to the NM by means of non-coding sequences of variable length known as matrix attachment regions or MARs. Yet there is no consensus sequence for a priori identification of MARs although they are generally rich in AT and repetitive sequences, and map to regions where the DNA is intrinsically curved or kinked and has a propensity for base unpairing [Ottaviani et al., 2008]. MARs are operationally classified in structural-constitutive, resistant to high-salt extraction and transient-functional, non-resistant to high-salt extraction [Razin, 2001; Maya-Mendoza et al., 2003]. The former high-salt resistant attachments are also known as true loop attachment

regions or LARs [Razin, 2001]. Therefore, not all potential MARs are actually bound to the NM or constitute LARs. There is evidence that when multiple copies of a specific MAR are present these are used in a selective fashion, indicating adaptability of the MAR sequence to serve as anchor only under certain conditions [Heng et al., 2004]. Fundamental processes of nuclear physiology such as DNA replication, transcription, and processing of primary transcripts occur at macromolecular complexes or factories organized upon the NM [Berezney and Wei, 1998; Cook, 1999; Anachkova et al., 2005]. Thus, the topological relationship between the DNA loops and the NM appears to be very important for nuclear physiology. Indeed the DNA–NM interactions define a higher order structure within the cell nucleus (NHOS).

As yet very little is known about the factors involved in selecting, establishing, and modulating the MAR/LAR–NM interactions. It has been suggested that the cell is a vector field in which the linked cytoskeleton–nucleoskelton may act as coordinated transducers of mechanical information [Aranda-Anzaldo, 1989]. Currently there is

Grant sponsor: CONACYT, México; Grant number: 48447-Q-25506; Grant sponsor: Universidad Autónoma del Estado de México, México; Grant number: 2212/2006.

*Correspondence to: Dr. Armando Aranda-Anzaldo, MD, PhD, Laboratorio de Biología Molecular, Facultad de Medicina, UAEMéx., Paseo Tollocan y Jesús Carranza s/n, Toluca, 50180, Edo. Méx., México.

E-mail: aaa@uaemex.mx

Received 25 October 2010; Accepted 27 October 2010 • DOI 10.1002/jcb.22943 • © 2010 Wiley-Liss, Inc.

Published online 22 November 2010 in Wiley Online Library (wileyonlinelibrary.com).

ample experimental evidence of the mechanical coupling between the cytoskeleton and the cell nucleus [Wang et al., 2009]. Some models predict that permanent changes in cell shape must lead to modified mechanical interactions within the cell and that this would lead to structural changes within the cell nucleus resulting in redefinition of structural DNA loop domains [Aranda-Anzaldo, 1989]. An experimental test of this hypothesis in which cultured cells were stably shifted from their original rhomboidal to a spindle-like shape led to reorganization of specific structural DNA loop domains, resulting in the substitution of previous LARs by new high-salt resistant DNA–NM interactions, suggesting that nuclear shape could be a major determinant for establishing the structural DNA–NM interactions [Martínez-Ramos et al., 2005].

In the present work we studied in a comparative fashion the NHOS in two primary cell types from the rat: hepatocytes and naive B lymphocytes, by analyzing the topological relationships between the NM and a set of eight short gene sequences located in six separate chromosomes and as such representing a coarse-grained, large-scale sample of the topological organization of nuclear DNA into structural loop domains. The choice of the cell types studied was based on the relative similarity of their rather spherical nuclear shape but also considering that such cells have different embryonic origin (endoderm for the hepatocytes and mesoderm for the B lymphocytes) as well as the fact that hepatocytes constitute a solid tissue while naive B lymphocytes are freely moving cells and that both types of cell are normally in a quiescent state (G0) and yet they preserve a proliferating potential that it is elicited under specific circumstances, such as partial hepatectomy or antigenic stimulation. Our results indicate that the organization of nuclear DNA into structural loop domains is cell-type specific since most of the gene sequences studied showed significant differences in their relative position to the NM according to cell type, refuting the working hypothesis that nuclear shape is the major determinant for DNA–NM interactions. However, such cell-type specific differences in the NHOS have no obvious correlation with the tissue-specific transcriptional activity of the corresponding genes, supporting the notion that permanent, structural DNA loops are different from the transient, functional DNA loops that may be associated with transcription.

MATERIALS AND METHODS

ANIMALS

Male Wistar rats weighing 200–250 g fed with food and water ad libitum were used for obtaining primary cells. All procedures involving animals were carried out in accordance with the official Mexican norm for production, care, and use of laboratory animals [NOM-062-ZOO-1999] and approved by the UAEMéx School of Medicine Committee on Bioethics.

PRIMARY CELLS

Primary rat hepatocytes were obtained from livers of male Wistar rats, using the protocol previously described [Maya-Mendoza et al., 2003]. Briefly, the livers were washed in situ by perfusion with PBS without Ca^{2+} and Mg^{2+} (PBS-A) 15 ml/min at 37°C for 5 min using a cannula (28–18 caliber needles) introduced in the portal vein or a

main portal branch. The cave vein was cut at the level of the kidneys in order to elute the liver content. Next the tissue was perfused with a solution of collagenase IV, Sigma (0.025% collagenase with 0.075% of CaCl_2 in Hepes buffer, pH 7.6) for 8 min. Viable hepatocytes were counted in a hemocytometer and used immediately for preparing nucleoids (see below). Primary naive B lymphocytes were obtained from the spleen of male Wistar rats. Briefly, the spleen was removed, fragmented and filtered through a mesh with pores of 400 μm in PBS-A. Total lymphocytes were purified from spleen extract by centrifugation at 2,100 rpm for 15 min at room temperature in a isotonic, preformed continuous gradient of Percoll 25%. Subsequently, quiescent B lymphocytes were obtained by marking with anti CD43-specific beads (rat CD43 microbeads, Miltenyi Biotec) and magnetic separation (MACS Separation columns, Miltenyi Biotec), according to the manufacturer instructions. Viable naive B lymphocytes were counted in a hemocytometer and used immediately for preparing nucleoids.

PREPARATION OF NUCLEOIDS

The DNA loops plus the nuclear substructure constitute a “nucleoid,” a very large nucleoprotein aggregate generated by gentle lysis of a cell at pH 8.0 in non-ionic detergent and the presence of high-salt concentration. Nucleoids were prepared as previously described [Cook et al., 1976; Maya-Mendoza and Aranda-Anzaldo, 2003], briefly: freshly isolated and washed hepatocytes and B lymphocytes were suspended in ice-cold PBS-A. Aliquots of 50 μl containing 3.5×10^5 hepatocytes and 5×10^5 B lymphocytes respectively, were gently mixed with 150 μl of a lysis solution containing 2.6 M NaCl, 1.3 mM EDTA, 2.6 mM Tris, 0.6% Triton X-100 (pH 8.0). After incubating 20 min at 4°C for hepatocytes and 15 min at 4°C for B lymphocytes, the mixture was overlaid on sucrose step gradients that contain 0.2 ml of 30% sucrose under 0.6 ml 15% sucrose. Both sucrose layers contained 2.0 M NaCl, 1.0 mM EDTA, 10 mM Tris, pH 8.0. The gradients were spun at 4°C in a microfuge for 4 min at 10,000 rpm (9,000g). The nucleoids form a white aggregate that usually sediments to the interface between the two layers of sucrose. The nucleoids were recovered in a volume ranging from 200 to 300 μl . The main aliquot was washed in 14 ml of PBS-A at 4°C for 5 min at 3,000 rpm (1,500g). The final nucleoid pellet was recovered in a volume ranging from 200 to 300 μl .

NUCLEOID FLUORESCENT HALO ASSAY

Hepatocyte or naive B lymphocyte nucleoids aliquots (10 μl) were deposited directly on a slide and stained with 10 μl of EB at 160 $\mu\text{g}/\text{ml}$ (final concentration 80 $\mu\text{g}/\text{ml}$) and examined by fluorescence microscopy after 30 s of DNA-halo expansion for assessing the nucleoid DNA integrity and supercoiling [Aranda-Anzaldo and Dent, 1997]. All procedures involving epifluorescence microscopy were carried out using an Olympus BX60 microscope fitted with an Evolution MP Color camera for image and video acquisition. Images and videos were processed with the Image-Pro Plus digital image analysis system Version 4.5 (Media-Cybernetics). Average DNA halo radii were estimated from the core nucleoid contour to the outer limit of the DNA halo using the image analysis software. For real-time nucleoid videos, selected representative nucleoids were focused

under phase contrast and a sequence of 30 fluorescent images was captured using the minimum possible time interval.

DNase I DIGESTION OF NUCLEOID SAMPLES

The washed nucleoids are pooled for setting up the DNase I digestion curves (1.8×10^6 nucleoids of hepatocytes and 2.5×10^6 nucleoids of B lymphocytes in 1.2 ml of PBS-A) and mixed with 5 ml of DNase I digestion buffer (10 mM $MgCl_2$, 0.1 mM dithiothreitol, 50 mM Tris at pH 7.2). Digestions were carried out at 37°C with 0.5 U/ml DNase I (Sigma). Each digestion time-point aliquot contains 3×10^5 nucleoids of hepatocytes or 5×10^5 nucleoids of B lymphocytes. Digestion reactions were stopped by adding 200 μ l of stop buffer (final EDTA concentration of 30 mM). The stop buffer contains 0.2 M EDTA and 10 mM Tris at pH 7.5. After digestion with DNase I, the NM-bound DNA was determined by spectrometry on aliquots of partially digested nucleoid samples that were washed and further handled as described previously [Maya-Mendoza and Aranda-Anzaldo, 2003]. The final nucleoid pellet was re-suspended in 200 μ l of double-distilled H_2O to be used directly as a template for PCR.

GENOMIC DNA PRIMERS

Distinct sets of primers were designed for establishing the topological positions relative to the NM of small target DNA sequences of genes expressed in hepatocytes and B lymphocytes. Important considerations were taken into account for designing the oligonucleotide pairs of primers so as to get primers with high specificity but able to perform efficient DNA amplification under the same PCR conditions (reactants concentrations, temperatures, times of each step, and number of cycles). All primer sets were designed with a length of 20–25 bp, G-C content between 50% and 55% (with a difference <3%), T_m of 55–60°C (with a difference <2°C), and PCR products of 250–500 bp (Table I). Secondary structures with $\Delta G < -1$ kcal/mol and dimers/duplexes with $\Delta G < -2$ kcal/mol were

avoided. Additionally, the specificity of each primer set was confirmed by the NCBI BLAST algorithm.

PCR AMPLIFICATION

Ten nanograms of NM-bound DNA of hepatocytes and B lymphocytes were used as template for PCR. PCR was carried out using 0.7 U GoTaq DNA polymerase (Promega), 1.5, 2.0, and 2.5 mM $MgCl_2$, 0.2 mM of each dNTP, and 0.1 μ M of each primer. Amplification was performed in an Applied Biosystems 2720 thermocycler and the same amplification program was used for all pairs of primers: initial denaturation step at 94°C for 5 min, denaturation step at 94°C for 45 s, annealing at 56°C for 30 s, and extension at 72°C for 1 min for 35 cycles, with a final extension at 72°C for 10 min. The identity of all the amplified sequences was confirmed by restriction analysis with the appropriate restriction enzymes. Amplified PCR products were electrophoresed on 2.5% agarose gels and visualized using ethidium bromide (EB) staining, recorded and analyzed using a Kodak ID Image Analysis Software 3.5 system. Amplicons were scored as positive or negative on partially digested nucleoid samples, depending on whether they are detectable or not by the software using the default settings.

RT-PCR

Total RNA from isolated hepatocytes and B lymphocytes was obtained using RNAqueous[®]-4PCR (Ambion). All RNA samples were quantified and normalized using spectrophotometric methods. Double-stranded cDNA was synthesized from extracted RNA using M-MVL reverse transcriptase (Promega) and random primers according to the manufacturer's protocol. Reverse transcription was performed using 500 ng of total RNA. The pairs of primers were designed complementary to sequences in the mRNA. All primer sets were designed with a length of 18–20 bp, G-C content between 50% and 55% (with a difference <3%), T_m of 55–60°C (with a difference <2°C), and PCR products of 250–700 bp (Table II). Secondary

TABLE I. Pairs of Primers Used for Amplification of Small Target Sequences Corresponding to Eight Different Genes Located in Six Separate Chromosomes Representing a Large-Scale Sample of the Nuclear Higher Order Structure (NHOS)

Amplicon	Forward primer	Reverse primer	Amplicon length (bp)	Chromosomal location
CD23	TAGGAGACGATGCTGCTGTGCA	CGTGGGAAGAGGATCAGACAAGAA	284	12p12
CD86	CCACTCTCAGATCCACATTCCT	CCAGGCTCTACGACTTCACAATGT	284	11
Lyn	CCCTCCAGCACAGTATGCAAA	CGGTGACTTCGGTTCAAAGCTA	277	20
Fyn	ACACAATGCTGATCTAGTCGTGGC	CACATCTGTGTTTCATCACTGTCCG	340	5
ALB	TGGCAAACATACGCAAGGGA	GCGAAACACACCCCTGGAAA	275	14
AFP	CCCAGGGTCAGAGTATATCAGTGC	CGCTGAACGTATGTCTGAGTCA	305	14
ACTIN	CGTAAAGACCTCTATGCCA	AGCCATGCCAAATGTGTCAT	473	12q11
COL1 A1	CATACCTGGGCCACACCAT	CTTGACITTCCTCTGGGA	261	10

TABLE II. Pairs of Primers Used for RT-PCR Amplification of cDNA Complementary to mRNA Sequences From Seven Target Genes

Amplicon	Forward primer	Reverse primer	Amplicon length
CD23	CTTACACAGCTGTGACCA	CCGTTCCCTTTGACATCAG	632
CD86	ATGCTGTTCTGTGAAGAG	AAGTCTTTCGATCAAACCTG	666
Lyn	GTAGATATGAAGACTAA	ATCTCCCAAGCATCTTTAT	677
Fyn	TGAAGGACGGGCTCTGAA	TGTAGCCTCTCTCCACCTG	380
ALB	ATACCCAGAAAGCACCTC	CACGAATTGTGCGAATGTCAC	436
AFP	CAGTGAGGAGAAACGGTCCG	ATGGTCTGTAGGGCTCGGCC	252
ACTIN	CGTAAAGACCTCTATGCCAA	AGCCATGCCAAATGTGTCAT	349

structures with $\Delta G < -1$ kcal/mol and dimers/duplexes with $\Delta G < -2$ kcal/mol were avoided. The same amplification program was used for all pairs of primers (10 pmol): initial denaturation step at 94°C for 5 min, denaturation step at 94°C for 45 s, annealing at 56°C for 1 min, and extension at 72°C for 1 min for 35 cycles, with a final extension at 72°C for 10 min. Additionally, the specificity of each primer set was confirmed by the NCBI BLAST algorithm. The identity of all the amplified sequences was confirmed by restriction analysis with the appropriate restriction enzymes. Amplified PCR products were electrophoresed on 2.5% agarose gels and visualized using EB staining, recorded and analyzed using a Kodak ID Image Analysis Software 3.5 system.

RESULTS

STABILITY OF THE NM AND THE DNA–NM INTERACTIONS IN NUCLEOIDS FROM HEPATOCYTES AND NAIVE B LYMPHOCYTES

The DNA loops plus the NM constitute a nucleoid. Under the conditions of lysis employed to generate nucleoids the DNA remains essentially intact but it lacks the nucleosome structure because of the dissociation of histones and other chromatin proteins; yet the naked DNA loops remain topologically constrained and supercoiled being attached to the NM [Cook et al., 1976; Roti-Roti et al., 1993]. Indeed, nucleoids are also known as nuclear halos since exposure of such structures to DNA-intercalating agents like EB leads to unwinding of the DNA loops that form a fluorescent DNA halo around the NM periphery. The EB acts as a molecular lever causing the unwinding of loop DNA and this process induces strong tearing forces that impinge upon the NM as the DNA rotates and expands during unwinding. Thus, the stability of the DNA–NM interactions and of the NM itself can be evaluated by exposing the corresponding nucleoids to a high concentration of EB since in certain types of nucleoids the EB-induced unwinding of loop DNA may result in tearing and release of DNA from the NM or even in the destruction of the NM framework [Martínez-Ramos et al., 2005; Maya-Mendoza et al., 2005]. Exposure of nucleoids from young–adult rat hepatocytes to EB (80 $\mu\text{g}/\text{ml}$) leads to complete unwinding of the DNA loops that form a homogeneous and well-defined halo around the NM periphery (Fig. 1B,C) and yet the NM framework (Fig. 1A,D) remains unperturbed after the EB-induced unwinding of loop DNA (Fig. 1A,D) indicating the presence of a large number of firm DNA attachments to a very stable NM. Similarly, most nucleoids from young–adult rat naive B lymphocytes display a well-defined halo around the NM after the exposure to EB (Fig. 1F,G) without affectation of the original NM framework (Fig. 1E,H). Nevertheless in the nucleoid samples from naive B lymphocytes there was always a subpopulation ($\leq 30\%$) that manifested various degrees of structural perturbation after exposure to EB going from partial or complete release of loop DNA from the NM up to eventual fragmentation of the NM framework. The subpopulation of fragile nucleoids was actually composed from a wide and varied array of fragility subtypes since reduction of the EB concentration from 80 to 40 $\mu\text{g}/\text{ml}$ resulted in a much reduced fraction of perturbed nucleoids but some B lymphocyte nucleoids were still destroyed after exposure to 10 $\mu\text{g}/\text{ml}$ of EB (data not shown).

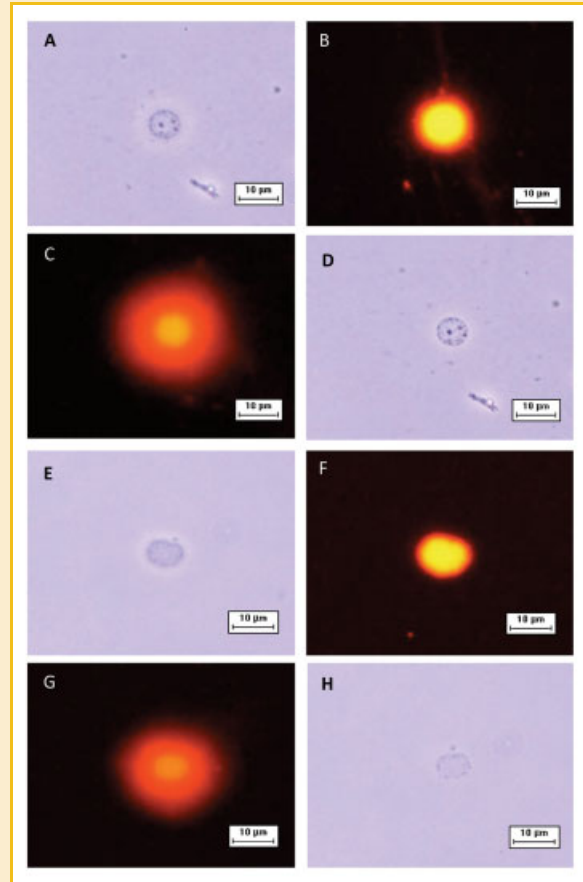


Fig. 1. Morphology and stability of the rat hepatocyte and naive B lymphocyte nucleoids. A: Phase contrast micrograph showing the typical spherical morphology of the nuclear matrix (NM) from a hepatocyte. B: Fluorescence micrograph of the same hepatocyte nucleoid as in A treated with 80 $\mu\text{g}/\text{ml}$ of ethidium bromide (EB). C: Formation of a homogeneous DNA halo by the relaxed DNA loops around the NM contour after 30 s of exposure to EB. D: Phase contrast micrograph of the same rat hepatocyte nucleoid after treatment with EB showing the unperturbed NM. E: Phase contrast micrograph showing the typical morphology of the nuclear matrix (NM) from a B lymphocyte. F: Fluorescence micrograph of the same B lymphocyte nucleoid treated with 80 $\mu\text{g}/\text{ml}$ of EB. G: Formation of a homogeneous DNA halo by the relaxed DNA loops around the NM contour after 30 s of exposure to EB. H: Phase contrast micrograph of the B lymphocyte nucleoid after treatment with EB. Note that after EB treatment the morphology of the NM is preserved in both types of nucleoids.

COMPARATIVE KINETICS OF DNase I DIGESTION OF LOOP DNA IN NUCLEOIDS FROM HEPATOCYTES AND NAIVE B LYMPHOCYTES

The naked DNA loops anchored to the NM are topologically equivalent to closed DNA circles. Under such condition the DNA molecule undergoes significant structural stress that is spontaneously dissipated by coiling the molecule upon its own axis thus achieving negative supercoiling in a similar fashion as a pulled house-telephone cord [Calladine et al., 2004]. Thus, the naked DNA loops display a gradient of supercoiling that goes from lower to higher from tip to base of the loop, save for the fact that the structural properties of MARs are such that they also function as buffers or sinks of negative supercoiling thus avoiding maximal supercoiling at the base of the loops [Benham et al., 1997]. A typical

DNA loop can be divided in four topological zones according to their relative proximity to the NM [Rivera-Mulia and Aranda-Anzaldo, 2010] each of these zones manifest and identifiable behavior when exposed to a non-specific nuclease like DNase I that is sensitive to the local DNA topology [Lewin, 1980]. We have previously shown that in nucleoid preparations the relative resistance of a given loop-DNA sequence to a limited concentration of DNase I is directly proportional to its proximity to the NM anchoring point [Maya-Mendoza and Aranda-Anzaldo, 2003; Maya-Mendoza et al., 2004; Rivera-Mulia and Aranda-Anzaldo, 2010] two main factors determine such property: (1) Steric hindrance resulting from the proteinaceous NM that acts as a physical barrier that relatively protects the naked loop DNA that is closer to the NM from endonuclease action. (2) The local degree of loop DNA supercoiling that is lower in the distal portions of the loop and higher in the regions proximal to the NM. Both factors only confer relative but not absolute DNase I resistance to loop DNA. Thus, in a large sample of nucleoids exposed to a limited concentration of DNase I there is a

consistent trend in which the loop-DNA sensitivity to the enzyme is inversely proportional to its distance relative to the NM and so distal regions of the loop are digested first while the regions closer to the NM are digested later. Indeed, it is known that the DNA deeply embedded within the NM is very resistant to DNase I action and there is a fraction corresponding to some 2% of the total DNA that is basically non-digestible even when exposed to high concentrations of the enzyme [Berezney and Buchholtz, 1981], likely to represent the regions that include the actual MARs (LARs) anchored to the NM.

In the corresponding DNase I digestion curves (Fig. 2) it is possible to identify three different phases [Rivera-Mulia and Aranda-Anzaldo, 2010]: the first corresponds to a relatively fast kinetics in which the DNA corresponding to the loop fraction distal to the NM is preferentially digested because in such a fraction minor DNA supercoiling is the only barrier to the endonuclease action. The second phase shows a slower kinetics of digestion resulting from a slower rate of supercoiling loss in the DNA proximal to the NM. The third is the longest and slowest phase resulting from the proximity

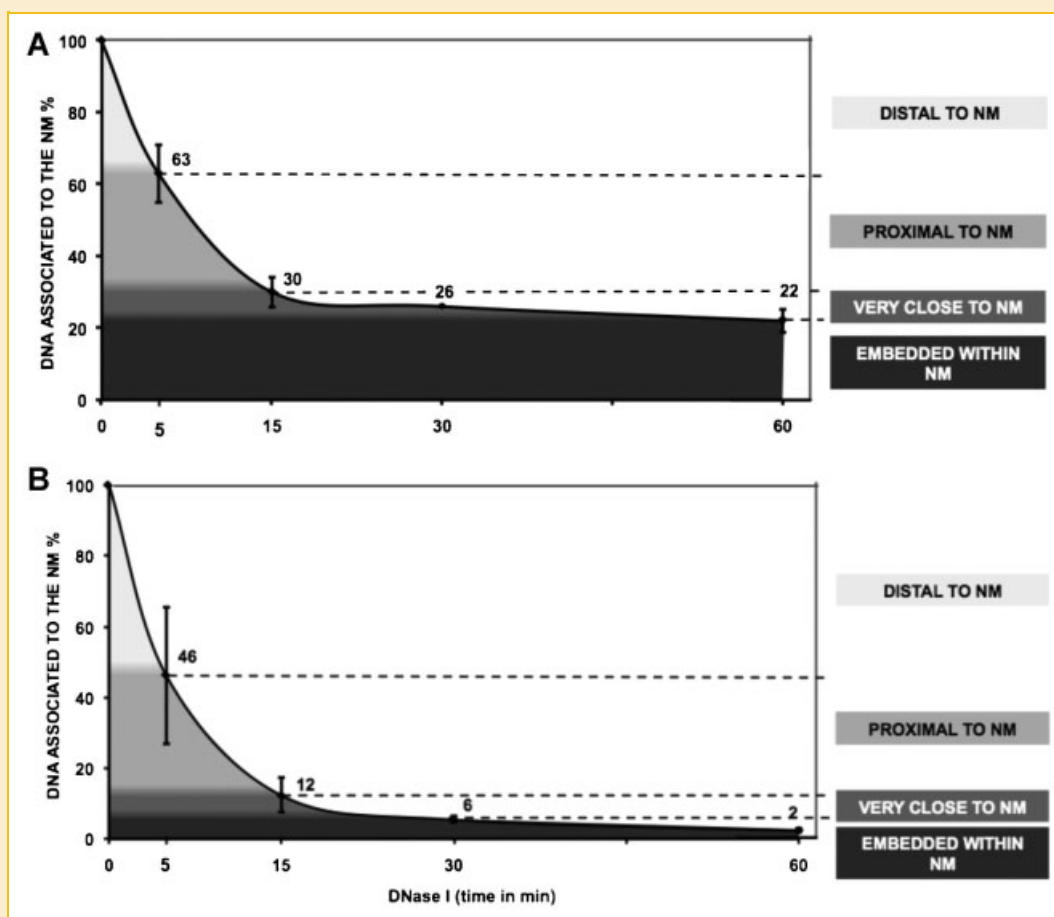


Fig. 2. Kinetics of DNase I digestion of loop DNA in nucleoids from hepatocytes and naive B lymphocytes. Nucleoids were treated with DNase I (0.5 U/ml). Each digestion time-point value corresponds to the average of independent experiments obtained from separate animals ($n = 4$ for hepatocytes, $n = 3$ for naive B lymphocytes). Bars indicate the corresponding SD. The topological zones relative to the NM correspond to decreasing percentages of total DNA bound to the NM. A: For hepatocytes: distal to NM (100–55% of total DNA), proximal to NM (55–26% of total DNA), very close to NM (26–19% of total DNA) and embedded within NM (19–0% of total DNA). The corresponding slopes are the following: 0–5 min = -7.4 ; 5–15 min = -3.3 ; 15–30 min = -0.3 ; 30–60 min = -0.1 . B: For naive B lymphocytes: distal to NM (100–27% of total DNA), proximal to NM (27–7% of total DNA), very close to NM (7–5% of total DNA), and embedded within NM (5–0% of total DNA). The corresponding slopes are the following: 0–5 min = -10.8 ; 5–15 min = -3.4 ; 15–30 min = -0.4 ; and 30–60 min = -0.1 .

between the loop DNA and the NM proteins that act as physical barriers against the free action of DNase I upon the loop DNA that is very close to the NM. Finally, there is a fraction of loop DNA that is resistant to DNase I even after long incubation times (the local slope of the digestion curve becomes very close to zero and remains unchanged in time), corresponding to the DNA that is actually embedded within the NM and so it is rather inaccessible to the limited concentration of enzyme used (Fig. 2). The kinetics of loop DNA digestion indicate that very different amounts of DNA are interacting with the NM in both kinds of nucleoids either as DNA tracts just embedded within the NM or as LARs directly bound to the NM, since in the hepatocytes some 20% of total DNA is embedded within the NM (Fig. 2A) while in the case of B lymphocytes only some 2% of total DNA is within the NM (Fig. 2B).

COMPARATIVE POSITIONAL MAPPING OF DNA SEQUENCES RELATIVE TO THE NM IN HEPATOCYTES AND NAIVE B LYMPHOCYTES

It is possible to exploit the aforementioned properties of loop DNA in order to map the position of any DNA sequence relative to the NM and so to determine its location within a given DNA-loop topological zone by coupling the specific kinetics of DNase I digestion (Fig. 2) with data from direct PCR amplification of the target sequences in NM-bound templates from partially digested nucleoid samples corresponding to the time-points of the DNase I digestion curve. The detailed methodology for such a positional mapping has already been published [Maya-Mendoza and Aranda-Anzaldo, 2003; Maya-Mendoza et al., 2004; Rivera-Mulia and Aranda-Anzaldo, 2010]. In order to establish whether the higher order structure in the cell nucleus (NHOS), corresponding to the

pattern of LARs and structural DNA loops, is similar or not between hepatocytes and naive B lymphocytes we carried out a comparative positional mapping relative to the NM of a set of target sequences (Table I) belonging to eight different genes: actin (*Act*) target located in exon 5–intron 5–exon 6, albumin (*Alb*) target located in the 5' flanking region of the gene, alpha-fetoprotein (*Afp*) target located in the 5' flanking region of the gene, CD23 target located in exon 1 of the gene, CD86 target located in exon 1 of the gene, collagen type 1 alpha-1 (*Col1A1*) target located in the 5' flanking region of the gene, Fyn tyrosine kinase (*Fyn*) target located in exon 1 of the gene, Lyn tyrosine kinase (*Lyn*) target located in exon 1 of the gene. The chosen genes are located in six separate rat chromosomes (Table I) and so they represent a sample of different chromosome territories within the cell nucleus [Meaburn and Misteli, 2007].

The results show that the target sequences mapped either to the distal or proximal regions relative to the NM in nucleoids from primary rat hepatocytes (Fig. 3 and Table III). However, with the exception of *Lyn* the same target sequences mapped to the region embedded within the NM in nucleoids from rat B lymphocytes (Fig. 4 and Table IV) indicating a dramatic difference in the NHOS between both primary cell types.

NO CORRELATION BETWEEN A GENE RELATIVE POSITION TO THE NM AND ITS TRANSCRIPTIONAL STATUS

In vivo transcription occurs at macromolecular complexes known as transcription factories that may be organized upon the NM [Berezney and Wei, 1998; Cook, 1999]. Earlier reports indicated that actively transcribed genes are preferentially associated with the NM [Small et al., 1985; Ramana-Murty et al., 1988] although it was unclear whether such an association is a precondition for transcription or it actually results from the act of transcription

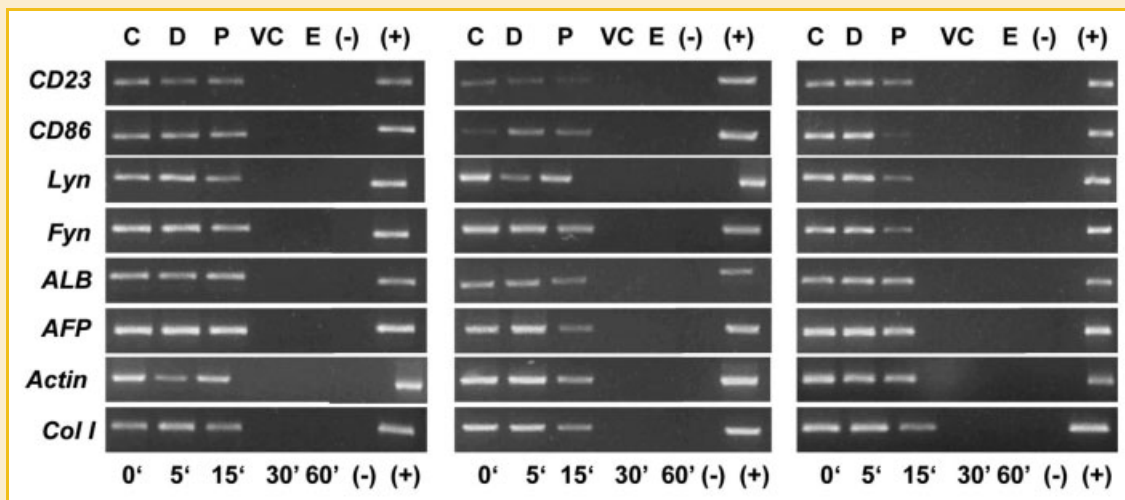


Fig. 3. Positional mapping relative to the NM of specific target DNA sequences in rat hepatocytes. Specific amplicons corresponding to the target sequences of eight genes (CD23, CD86, Lyn, Fyn, ALB, AFP, Actin, and Col1A1) whose relative position to NM was mapped in nucleoids from rat hepatocytes. Nucleoids from isolated hepatocytes were treated with DNase I (0.5 U/ml) for 0, 5, 15, 30, and 60 min and further processed for direct PCR amplification of the target sequence in the residual NM-bound templates. The amplicons were visualized in 2% agarose gels stained with ethidium bromide. The amplicons were located in different topological zones relative to NM in agreement with the specific kinetics of nucleoid DNA digestion (Fig. 2A). The presence of the target sequence in the residual NM-bound DNA of the partially digested samples was scored as positive (independently of the actual intensity of the amplicon band) if the amplicon was detected by the Kodak 1D Image Analysis Software version 3.5. C, control; D, distal to NM; P, proximal to NM; VC, very close to NM; E, embedded within NM; (-), negative control without DNA; (+), positive control with genomic DNA. The amplicon patterns were consistently reproduced in separate experiments with samples from independent animals, n = 3.

TABLE III. Location of the Target-Gene Sequences Within the Specific Topological Zones Relative to the NM in Nucleoids From Hepatocytes

Amplicon	Distal to NM	Proximal to NM	Very Close to NM	Embedded within NM
CD23	+	+	-	-
CD86	+	+	-	-
Lyn	+	+	-	-
Fyn	+	+	-	-
ALB	+	+	-	-
AFP	+	+	-	-
ACTIN	+	+	-	-
Col 1 A1	+	+	-	-

(+) Indicates that the amplicon was detected by the image analysis software; (-) indicates that the amplicon was not detected by the image analysis software. Amplification results were exactly the same in at least three separate experiments

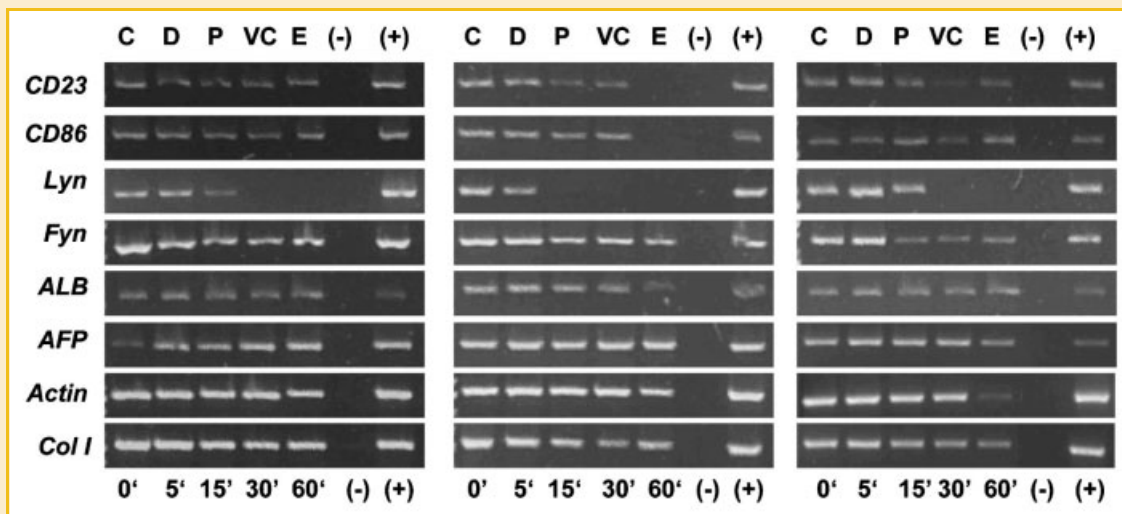


Fig. 4. Positional mapping relative to the NM of specific target DNA sequences in rat naive B lymphocytes. Specific amplicons corresponding to the target sequences of the eight genes studied (CD23, CD86, Lyn, Fyn, ALB, AFP, Actin, and Col1A1) whose relative position to NM was mapped in nucleoids from rat B lymphocytes. Nucleoids from isolated lymphocytes were treated with DNase I (0.5 U/ml) for 0, 5, 15, 30, and 60 min and further processed for direct PCR amplification of the target sequence in the residual NM-bound templates. The amplicons were visualized in 2% agarose gels stained with EB. The amplicons detected by PCR were located in different topological zones relative to NM in agreement with the specific kinetics of nucleoid DNA digestion (Fig. 2B). The presence of the target sequence in the residual NM-bound DNA of the partially digested samples was scored as positive (independently of the actual intensity of the amplicon band) if the amplicon was detected by the Kodak 1D Image Analysis Software version 3.5. C, control; D, distal to NM; P, proximal to NM; VC, very close to NM; E, embedded within NM; (-), negative control without DNA; (+), positive control with genomic DNA. The amplicon patterns were consistently reproduced in separate experiments with samples from independent animals, n = 3.

TABLE IV. Location of the Target-Gene Sequences Within the Specific Topological Zones Relative to the NM in Nucleoids From Naive B Lymphocytes

Amplicon	Distal to NM	Proximal to NM	Very close to NM	Embedded within NM
CD23	+	+	+	+
CD86	+	+	+	+
Lyn	+	+	-	-
Fyn	+	+	+	+
ALB	+	+	+	+
AFP	+	+	+	+
ACTIN	+	+	+	+
Col 1 A1	+	+	+	+

(+) Indicates that the amplicon was detected by the image analysis software; (-) indicates that the amplicon was not detected by the image analysis software. Amplification results were exactly the same in at least three separate experiments.

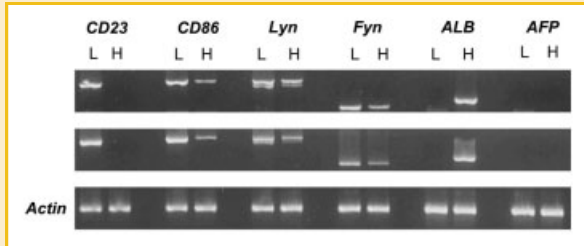


Fig. 5. Expression of seven target genes monitored by RT-PCR. The specific amplicons of the target cDNA sequences and their corresponding expression patterns in naive B lymphocytes and hepatocytes are shown. The expression of Actin is shown as positive control for both cellular types. L = B lymphocytes; H = hepatocytes. The amplicon patterns were consistently reproduced in separate experiments with samples from independent animals, $n = 3$.

itself [Stein et al., 1995]. We performed RT-PCR experiments in order to assess if there was a correlation between the position of the target genes relative to the NM and their transcriptional status. The results show that there is no obvious correlation between position relative to the NM and transcription. For example the gene *Fyn* is similarly transcribed in both hepatocytes and B lymphocytes (Fig. 5) despite the fact that in the hepatocytes such a gene is only proximal to the NM while being embedded into the NM in the case of B lymphocytes (Tables III and IV). *Afp* is not expressed in both cell types (Fig. 5) despite the obvious positional difference relative to the NM of such a gene in both cell types (Tables III and IV). Moreover, *Act* is constitutively expressed in both cell types regardless of its position relative to the NM (Fig. 5 and Tables III and IV).

DISCUSSION

The DNA of each chromosome constitutes a rather continuous double-stranded fiber in which each strand has a rigid helical backbone resulting from the strong phosphodiester bonds between the deoxyribose sugars of thousands of nucleotides along the strand, whereas the weak hydrogen bonds between the nitrogenous bases in the anti-parallel strands can be broken and re-established quite easily. Thus, the torsional stress of the long DNA molecule along its axis may be dissipated by breaking the hydrogen bonds between both strands, yet by looping and supercoiling along its axis DNA can dissipate the stress without compromising its structural integrity [Calladine et al., 2004]. Hence the topological interactions DNA–NM that result in a large number of structural DNA loops in the interphase nucleus are a natural answer to a structural stress problem posed by the intrinsic configuration of DNA. In principle, both the genomic nucleotide sequence and the karyotype are the same in all somatic cell types from a given mammal, thus it could be expected that the set of structural DNA–NM interactions would be rather similar in different cell types of the rat. Nevertheless, we have previously determined that the organization of a specific genomic region, the locus of the rat-albumin gene family, into structural DNA loops is remarkably different between primary hepatocytes and naive B lymphocytes [Rivera-Mulia and Aranda-Anzaldo, 2010]. Others have shown significant differences in the DNA loop

organization of the chicken alpha-globin gene between erythroid and lymphoid cell lines [Ioudinkova et al., 2005], suggesting that the NHOS might be cell-type specific. Indeed, the experiments described in the present work indicate that on a coarse-grained, large-scale the same genomic DNA interacts differentially with the NM according to cell type, hence the organization of the genome into structural looped domains is cell-type specific at least in the two cases studied. This conclusion can be reasonably established considering that any DNA sequence that is not an actual MAR/LAR must be located somewhere along a particular structural DNA loop and as such it must have a specific position relative to the NM where the loops are anchored. Hence, if the position relative to the NM of a given DNA sequence is different in two different cell types, as it was mostly the case in the present study, this can only be the consequence of a differential pattern of structural attachments of the DNA to the NM according to cell type.

A very limited number of specific proteins have been identified that participate in binding of DNA to the NM in a sequence-specific fashion [Tsutsui et al., 2005]. However, given that there are no MAR consensus sequences and yet the structural DNA–NM interactions occur on a grand scale, these facts imply that such interactions are the result of indirect readout effects between DNA and NM proteins thus not equivalent to the direct readout interactions between transcription factors and specific DNA-functional groups [Zhang et al., 2004]. Such protein–DNA indirect readouts depend on DNA shape (that is also dependent on nucleotide sequence) and overall DNA mechanical properties such as curvature, helical twist, and bending and torsional flexibilities [Calladine et al., 2004; Zhang et al., 2004]. The composition of the NM varies significantly among cell types even though there is a set of NM proteins common to all cell types [Fey and Penman, 1988; Stuurman et al., 1990]. This fact creates cell-type-specific conditions for developing stable interactions between the genomic DNA and the NM. The three nuclear lamins A, B, and C are major components of the NM from most mammalian cells, but it is well established that mammalian B lymphocytes either do not express lamin A/C or it is present in negligible amounts [Röber et al., 1990; Gerner and Saueremann, 1999]. This implies that the NM of B lymphocytes is less dense than that of hepatocytes and as such it may explain why a significantly lesser amount of total DNA is protected from DNase I in B lymphocyte nucleoids (Fig. 2B). Nevertheless, our experiments indicate that most B lymphocytes have a large number of stable DNA–NM interactions similarly to the hepatocytes (Fig. 1) and that the resulting DNA loops display a significant degree of supercoiling (Figs. 1 and 2). This evidence further contradicts earlier reports suggesting that quiescent B lymphocytes contain a large number of DNA strand breaks compared to other cell types [Johnstone, 1984; Kaplan et al., 1987], since high numbers of strand breaks should cause the spontaneous loss of loop DNA supercoiling [Aranda-Anzaldo, 1992; Aranda-Anzaldo and Dent, 1997]. Indeed, previous studies have already disproved that B lymphocytes are truly riddled with DNA strand breaks as it became clear that the native, circulating B lymphocytes have no excess of DNA breaks but that such breaks are induced during the cultivation of such cells in vitro [Boerrigter et al., 1989; Jostes et al., 1989; Moskaleva, 1990].

It has been suggested that cell differentiation and the corresponding cell-type-specific transcriptional profile may have a deeper structural basis resulting from differential patterns of DNA loops attached to the NM [Aranda-Anzaldo, 1989] this was based on early evidence that actively transcribed genes were preferentially associated with the NM [Small et al., 1985; Ramana-Murty et al., 1988] and further supported by the fact that transcription occurs at molecular complexes likely to be organized upon the NM [Jackson and Cook, 1985; Berezney and Wei, 1998; Cook, 1999]. Nevertheless, more recent work has been able to distinguish the interactions DNA–NM into those rather permanent and resistant to high-salt extraction and those rather transient and not-resistant to high-salt extraction [Razin, 2001; Maya-Mendoza et al., 2003]. It has already been established that a single transcriptional unit can be organized into several structural DNA loops [Iarovaia et al., 2004] and there are several reports indicating that transcriptional status of a given gene is independent of the gene relative position to the NM when dealing with nuclear preparations displaying structural DNA loops [Maya-Mendoza and Aranda-Anzaldo, 2003; Maya-Mendoza et al., 2003, 2004, 2005] as it was the case in the present report (Fig. 5 and Tables III and IV). However, it may also be the case that transient functional DNA loops are actually formed as a requirement for or in association with transcription that may occur associated or not with the NM [Iarovaia et al., 2005, 2009]. Yet our experimental system only detects those loops resistant to high-salt extraction and the relative position to the NM of the genes present in such structural loops is clearly not correlated with the transcriptional status of the genes.

It is known that replication and transcription occur at factories organized upon the NM [Cook, 1999; Anachkova et al., 2005; Mitchell and Fraser, 2008]. However, replication and transcription factories never co-localize since they occupy distinct but rather fixed sites within the cell nucleus [Wei et al., 1998]. Transcription occurs at factories organized in nuclear regions that do not imply the genetic continuity of the genes being transcribed, hence genes from separate chromosomes can be transcribed in the same transcription factory [Mitchell and Fraser, 2008]. On the other hand, varied evidence suggests that structural DNA loops may correspond to the actual subdivision of the genome into replication units [Razin, 2001] and that the NM performs a fundamental role as a structural organizer of DNA replication [Anachkova et al., 2005]. Furthermore, recent evidence indicates that the spatial continuity of the replication foci correlates with the genetic continuity of adjacent replicon clusters along chromosomes [Maya-Mendoza et al., 2010] thus supporting the notion that sets of adjacent structural DNA loops correspond to the actual replicon clusters *in vivo*. We have shown that in primary hepatocytes synchronized *in vivo* for DNA replication the DNA sequences located within the structural DNA loops move in a sequential fashion during the S phase, as if reeled in, towards the NM during DNA replication and later on return to their original position in the newly quiescent cells [Maya-Mendoza et al., 2003; Rivera-Mulia et al., submitted]. These facts support the notion that DNA replicates *in vivo* by reeling through replication factories located on the NM [Cook, 1999] and that the structural DNA loops are the actual replicons. However, there is no obvious reason why the replicons should be differentially organized in different cell

types given that the genome is basically of the same size in the different somatic cell types from the same organism.

In any case, the local spatial configuration of DNA into structural loops constitutes the starting point for any further refinement or modification of such a configuration by chromatin proteins and epigenetic mechanisms affecting chromatin structure. However, chromatin as such plays no role in determining the structural DNA loop organization since chromatin proteins are completely eliminated by the high-salt extraction and yet stable DNA–NM interactions persist in the resulting nucleoid preparations. The organization of the genome into structural DNA loops must be highly relevant for both replication and transcription since besides the evidence that the structural DNA loops correspond to the actual replicons *in vivo*, the pattern of such loops may also determine the limits of further local structural changes that may be associated with chromatin modifications resulting in transcription-related interactions between loop DNA and protein complexes organized upon the NM [Davie, 1996; Cook, 1999]. The nucleotype has been defined as those characters of nuclear DNA that may affect the phenotype independently of the information encoded in such a DNA, like the C-value that correlates with overall cell-cycle length [Bennett, 1977]. It has been suggested that besides such species-specific nucleotypic characters there could be tissue-specific nucleotypic characters [Aranda-Anzaldo, 1989]. Hence a differential organization of replicons according to cell type may be a tissue-specific nucleotypic character.

ACKNOWLEDGMENTS

While doing this work Claudia Trevilla-García was a CONACYT Research Scholar within the Graduate Program in Biomedical Sciences at IFC-UNAM, México.

REFERENCES

- Anachkova B, Djeliova V, Russev G. 2005. Nuclear matrix support of DNA replication. *J Cell Biochem* 96:951–961.
- Aranda-Anzaldo A. 1989. On the role of chromatin higher-order structure and mechanical interactions in the regulation of gene expression. *Speculat Sci Technol* 12:163–176.
- Aranda-Anzaldo A. 1992. Altered chromatin higher-order structure in cells infected by herpes simplex virus type 1. *Arch Virol* 124:245–253.
- Aranda-Anzaldo A, Dent MAR. 1997. Loss of DNA-loop supercoiling and organization in cells infected by herpes simplex virus type 1. *Res Virol* 149:195–208.
- Benham C, Kohwi-Shigematsu T, Bode J. 1997. Stress-induced duplex destabilization in scaffold/matrix attachment regions. *J Mol Biol* 277:181–196.
- Bennett MD. 1977. The time and duration of meiosis. *Philos Trans R Soc London B Biol Sci* 277:201–226.
- Berezney R, Buchholtz LA. 1981. Dynamic association of replicating DNA fragments with the nuclear matrix of regenerating liver. *Exp Cell Res* 132:1–13.
- Berezney R, Wei X. 1998. The new paradigm: Integrating genomic function and nuclear architecture. *J Cell Biochem* 30–31:238–242.
- Boerrigter ME, Mullart E, van Der Schans GP, Vijg J. 1989. Quiescent human peripheral blood lymphocytes do not contain a sizeable amount of pre-existent DNA single-strand breaks. *Exp Cell Res* 180:569–573.

- Calladine CR, Drew HR, Luisi BF, Travers AA. 2004. Understanding DNA. London: Elsevier-Academic Press. pp 94–138.
- Cook PR. 1999. The organization of replication and transcription. *Science* 282:1790–1795.
- Cook PR, Brazell I, Jost E. 1976. Characterization of nuclear structures containing superhelical DNA. *J Cell Sci* 22:303–324.
- Davie JR. 1996. Histone modifications, chromatin structure and the nuclear matrix. *J Cell Biochem* 62:149–157.
- Fey EG, Penman S. 1988. Nuclear matrix proteins reflect cell type of origin in cultured human cells. *Proc Natl Acad Sci USA* 85:121–125.
- Gerner C, Sauer mann G. 1999. Nuclear matrix proteins specific for subtypes of human hematopoietic cells. *J Cell Biochem* 72:470–482.
- Heng HHQ, Goetze S, Ye JC, Liu G, Stevens JB, Bremer SW, Wykes SM, Bode J, Krawetz SA. 2004. Chromatin loops are selectively anchored using scaffold/matrix-attachment regions. *J Cell Sci* 117:999–1008.
- Iarovaia OV, Bystritsky A, Ravcheev D, Hancock R, Razin SV. 2004. Visualization of individual DNA loops and a map of loop domains in the human dystrophin gene. *Nucleic Acids Res* 32:2079–2086.
- Iarovaia OV, Akopov SB, Nikolaev LG, Sverdlov ED, Razin SV. 2005. Induction of transcription within chromosomal DNA loops flanked by MAR elements causes an association of loop DNA with the nuclear matrix. *Nucleic Acids Res* 33:4157–4163.
- Iarovaia OV, Borounova VV, Philonenko ES, Kantidze OL, Vassetzky YS, Razin SV. 2009. In embryonic chicken erythrocytes actively transcribed alpha globin genes are not associated with the nuclear matrix. *J Cell Biochem* 106:170–178.
- Ioudinkova E, Petrov A, Razin SV, Vassetzky YS. 2005. Mapping long-range chromatin organization within the chicken alpha-globin gene domain using oligonucleotide DNA arrays. *Genomics* 85:143–151.
- Jackson DA, Cook PR. 1985. Transcription occurs at a nucleoskeleton. *EMBO J* 4:919–925.
- Johnstone AP. 1984. Rejoining of DNA strand breaks is an early nuclear event during stimulation of quiescent lymphocytes. *Eur J Biochem* 140:41–46.
- Jostes R, Reese JA, Cleaver JE, Molero M, Morgan WF. 1989. Quiescent human lymphocytes do not contain DNA strand breaks detectable by alkaline elution. *Exp Cell Res* 182:513–520.
- Kaplan JG, Brown DL, Chaly N, Greer WL, Prasad KV, Severini A, Sahai BM. 1987. Structural and evolutionary implications of the packaging of DNA for differentiation and proliferation in the lymphocyte. *J Mol Evol* 126:173–179.
- Lewin B. 1980. Gene expression. New York: John Wiley and Sons. pp 360–362.
- Martínez-Ramos I, Maya-Mendoza A, Gariglio P, Aranda-Anzaldo A. 2005. A global but stable change in HeLa cell morphology induces reorganization of DNA structural loop domains within the cell nucleus. *J Cell Biochem* 96:79–88.
- Maya-Mendoza A, Aranda-Anzaldo A. 2003. Positional mapping of specific DNA sequences relative to the nuclear substructure by direct polymerase chain reaction on nuclear matrix-bound templates. *Anal Biochem* 313:196–207.
- Maya-Mendoza A, Hernández-Muñoz R, Gariglio P, Aranda-Anzaldo A. 2003. Gene positional changes relative to the nuclear substructure correlate with the proliferating status of hepatocytes during liver regeneration. *Nucleic Acids Res* 31:6168–6179.
- Maya-Mendoza A, Hernández-Muñoz R, Gariglio P, Aranda-Anzaldo A. 2004. Gene positional changes relative to the nuclear substructure during carbon tetrachloride-induced hepatic fibrosis in rats. *J Cell Biochem* 93:1084–1098.
- Maya-Mendoza A, Hernández-Muñoz R, Gariglio P, Aranda-Anzaldo A. 2005. Natural ageing in the rat liver correlates with progressive stabilisation of DNA-nuclear matrix interactions and withdrawal of genes from the nuclear substructure. *Mech Ageing Dev* 126:767–782.
- Maya-Mendoza A, Olivares-Chauvet P, Shaw A, Jackson DA. 2010. S phase progression in human cells is dictated by the genetic continuity of DNA foci. *PLoS Genet* 6:e1000900.
- Meaburn KJ, Misteli T. 2007. Cell biology: Chromosome territories. *Nature* 445:379–381.
- Mika S, Rost B. 2005. NMPdb: Database of nuclear matrix proteins. *Nucleic Acids Res* 33:D160–D163.
- Mitchell JA, Fraser P. 2008. Transcription factories are nuclear subcompartments that remain in the absence of transcription. *Genes Dev* 22:20–25.
- Moskaleva E. 1990. Effects of lymphokines on DNA structure of in vitro cultured human lymphocytes. Connection with cAMP and oligoadenylate synthase systems. *Biull Eksp Biol Med* 110:417–419.
- Nickerson JA. 2001. Experimental observations of a nuclear matrix. *J Cell Sci* 114:463–474.
- Ottaviani D, Lever E, Takousis P, Sheer D. 2008. Anchoring the genome. *Genome Biol* 9:201.
- Ramana-Murty CV, Mancini MA, Chatterjee B, Roy AK. 1988. Changes in transcriptional activity and matrix association of the $\alpha 2\mu$ -globulin gene family in the rat liver during maturation and aging. *Biochem Biophys Acta* 949:23–34.
- Razin SV. 2001. The nuclear matrix and chromosomal DNA loops: Is there any correlation between partitioning of the genome into loops and functional domains? *Cell Mol Biol Lett* 6:59–69.
- Rivera-Mulia JC, Aranda-Anzaldo A. 2010. Determination of the *in vivo* structural DNA loop organization in the genomic region of the rat albumin locus by means of a topological approach. *DNA Res* 17:23–35.
- Röber RA, Sauter H, Weber K, Osborn M. 1990. Cells of the immune and hematopoietic system of the mouse lack lamins A/C: Distinction versus other somatic cells. *J Cell Sci* 95:587–598.
- Roti-Roti JL, Wright WD, Taylor YC. 1993. DNA loop structure and radiation response. *Adv Radiat Biol* 17:227–259.
- Small DS, Nelkin B, Vogelstein B. 1985. The association of transcribed genes with the nuclear matrix of *Drosophila* cells during heat shock. *Nucleic Acids Res* 7:2413–2431.
- Stein GS, van Wijnen AJ, Stein J, Lian JB, Montecino M. 1995. Contributions of nuclear architecture to transcriptional control. *Int Rev Cytol* 162A:251–278.
- Stuurman N, Meijne AML, van Der Pol AJ, de Jong L, van Driel R, van Renswoude J. 1990. The nuclear matrix from cells of different origin. *J Biol Chem* 265:5460–5465.
- Tsutsui KM, Sano K, Tsutsui K. 2005. Dynamic view of the nuclear matrix. *Acta Med Okayama* 59:113–120.
- Wang N, Tytell JD, Ingber DE. 2009. Mechanotransduction at a distance: Mechanically coupling the extracellular matrix and the nucleus. *Nat Rev Mol Cell Biol* 10:75–82.
- Wei X, Samarabandu J, Devdhar RS, Siegel AJ, Acharya R, Berezney R. 1998. Segregation of transcription and replication sites into higher order domains. *Science* 281:1502–1505.
- Zhang Y, Xi Z, Hegde RS, Shakked Z, Crothers DM. 2004. Predicting indirect readout effects in protein-DNA interactions. *Proc Natl Acad Sci USA* 101:8337–8341.